SYNTHESIS, CHARACTERIZATION AND CATALYTIC PERFORMANCE OF Cu/ZnO/SBA-15 FOR HYDROGENATION OF CARBON DIOXIDE TO METHANOL

NURUL AINI BINTI MOHAMED RAZALI

UNIVERSITI SAINS MALAYSIA

2014

SYNTHESIS, CHARACTERIZATION AND CATALYTIC PERFORMANCE OF Cu/ZnO/SBA-15 FOR HYDROGENATION OF CARBON DIOXIDE TO METHANOL

by

NURUL AINI BINTI MOHAMED RAZALI

Thesis submitted in fulfillment of the requirement
For the degree of
Doctor of Philosophy

Jun 2014

ACKNOWLEDGEMENT

First of all I would like to thank my supervisor, Prof. Dr. Abdul Rahman Mohamed, for his excellent guidance and support during my studies. My heartfelt thanks to my co-supervisors, Prof. Dr. Subhash Bhatia and Associate Prof. Dr. Lee Keat Teong for their incessant support, guidance and encouragement. Special thanks to Dr. Maedah Mohammadi for her invaluable discussion and help rendered throughout this research work.

I would like to thank to all the laboratory technicians and administrative staffs in the School of Chemical Engineering who have provide their help, particularly Mrs. Aswani Mohamad, Mrs Nurul Hidayah, Mr Syamsul Hidayat, Mr Roqib, Mr Faiza and Mr Arif.

I am also grateful to all the members of postgraduate students: Salwa, Henry, Khim May, Azreen, Husna, Mernoush, and others who have helped me through the thesis.

I am indeed very thankful to my loving husband, Mohammad Edziani Rosali, my prince and princess, Muhammad Nu'man and Aisyah Maisarah, my dearest mum and dad, Sharifah Normadiah Mamat and Mohamed Razali Mahmood, as well as my brothers and sisters. They are always on my side, riding along with my ups and downs.

Last but not least, I would like to thank Ministry of Higher Education and Universiti Malaysia Pahang for the financial support during my study. LRGS grant and RU team grant for financial support for this project.

TABLE OF CONTENTS

		Page
ACKNOWLEDGEMENT		ii
TABLE OF CONTENTS		iv
LIST OF TABLES		viii
LIST OF FIGURES		x
LIST OF ABBREVIATIONS		xiv
LIST OF SYMBOLS		xv
ABSTRAK		xvii
ABSTRACT		xix
CHAPTER 1 - INTRODUCTION		1
1.1	Global Warming	1
1.2	CO_2 in atmosphere	3
1.3	CO_2 conversion for global sustainability	4
1.4	CO_2 hydrogenation to CH_3OH	5
1.5	Santa Barbara Amorphous (SBA-15)	6
1.6	Problem statement	6
1.7	Objectives	9
1.8	Scopes of the work	10
1.9	Outline of thesis	11

CHAPTER 2 - LITERATURE REVIEW

2.1	Santa Barbara Amorphous 15 (SBA-15)	12
2.2	Synthesis method of SBA-15	17
2.3	Metallic Copper (Cu) and Zinc Oxide (ZnO)	20
	2.3.1 ZnO properties and applications	20
	2.3.2 Cu properties and applications	21
2.4	Roles of Cu and ZnO in CH_3OH synthesis from CO_2 hydrogenation	23
2.5	Synthesis method of metallic catalyst	25
	2.5.1 Synthesis of metallic catalyst by reflux method	26
2.6	CH_3OH production from CO_2 hydrogenation	29

2.6.1 Properties and applications of CH_3OH 29
2.6.2 Properties and applications of CO_2 33
2.7 Heterogeneous catalysts for CO_2 hydrogenation to CH_3OH 36
2.7.1 Cu/ZnO 36
2.7.2 Multicomponent catalysts 38

CHAPTER 3 - MATERIALS AND METHODS 48
3.1 Chemicals, gases and equipment 48
3.2 Overall experiment flowchart 51
3.3 Catalyst synthesis 52
3.3.1 Synthesis of SBA-15 52
3.3.2 Synthesis of CuO 53
3.3.3 Synthesis of Cu/ZnO 53
3.3.3 Synthesis of Cu/SBA-15 53
3.3.4 Synthesis of ZnO/SBA-15 54
3.3.5 Synthesis of bimetallic/SBA-15 55
3.4 Catalyst characterization techniques 57
3.4.1 X-ray diffraction (XRD) 57
3.4.2 Nitrogen adsorption 57
3.4.3 Thermogravimetric analysis (TGA) 57
3.4.4 Scanning electron microscopy (SEM) 58
3.4.5 Energy dispersive X-ray analysis (EDX) 58
3.4.6 Transmission electron microscopy (TEM) 58
3.4.7 Hydrogen-temperature programmed reduction (H_2-TPR) 59
3.5 Description of experimental set-up 59
3.5.1 Gas mixing system 62
3.5.2 Reactor system 62
3.5.3 Analysis system 65
3.6 Catalytic activity test for hydrogenation of CO_2 to CH_3OH 66
3.6.1 Blank test 66
3.6.2 Activity of SBA-15 support 67
3.6.3 Screening of the catalysts 67
3.6.4 Process optimization study 68

3.6.5 Activation energy 69
3.6.6 Catalyst stability 70
3.6.5 Products analysis 70

CHAPTER 4 - RESULTS AND DISCUSSION 73

4.1 Chapter overview 73
4.2 SBA-15 as support 73
  4.2.1 Characterization of the calcined SBA-15 74
  4.2.2 Summary 80
4.3 Preliminary study on the catalytic hydrogenation of CO_2 to CH_3OH 81
  4.3.1 Blank test 81
  4.3.2 Catalytic SBA-15 performance 82
4.4 Identifying the SBA-15 role 82
  4.4.1 Characterization 83
  4.4.2 Catalytic activity 86
  4.4.3 Summary 88
4.5 The role of Cu or ZnO 88
  4.5.1 Characterization 89
  4.5.2 Catalytic activity 92
  4.5.3 Summary 93
4.6 Effect of Cu/ZnO and their arrangement loading on SBA-15 94
  4.6.1 Characterization 95
  4.6.2 Catalytic activity 103
  4.6.3 Summary 106
4.7 Proposed reaction mechanism 107
4.8 Effect of Cu amount loading 111
  4.8.1 Characterization 111
  4.8.2 Catalytic activity 117
  4.8.3 Summary 121
4.9 Effect of ZnO amount loading 121
  4.9.1 Characterization 122
  4.9.2 Catalytic activity 127
  4.9.3 Summary 132

4.10 Process study and analysis 133
4.10.1 Effect of reaction pressure 134
4.10.2 Effect of reaction temperature 137
4.10.3 Effect of total GHSV 142
4.10.4 Summary 145
4.11 Activation energy 146
4.12 Catalyst stability 150

CHAPTER 5 152
5.1 Conclusions 152
5.2 Recommendations 154

REFERENCES 156

APPENDIX A 171

APPENDIX B 172

APPENDIX C 173

LIST OF PUBLICATIONS 174

LIST OF TABLES

		Page
Table 2.1	Properties of ZnO (Wikipedia. org, 2013)	21
Table 2.2	Properties of Cu (Wikipedia. org, 2013).	23
Table 2.3	Various heterogeneous catalysts for CH_3OH synthesis from CO_2 hydrogenation	45
Table 3.1	List of used chemicals, reagents and gases	49
Table 3.2	List of used equipment	50
Table 3.3	Definition of catalyst symbols	52
Table 3.4	Gas chromatography retention time data of the components	66
Table 3.5	Catalysts used in screening process	68
Table 3.6	Process study parameters for hydrogenation of CO_2 to CH_3OH	69
Table 4.1	Nitrogen adsorption parameters for calcined SBA-15 support	75
Table 4.2	CO_2 conversion recorded in a blank test study. Reaction condition: GHSV= 2400 h^{-1}; H_2/CO_2= 3; t= 3 h	81
Table 4.3	CO_2 conversion over SBA-15 support Reaction condition: GHSV= 2400 h^{-1}, H_2/CO_2= 3; t= 3 h	82
Table 4.4	BET surface area of Cu and Cu/SBA-15 catalyst	84
Table 4.5	BET surface area of calcined SBA-15, 10Cu/SBA-15 and 10Zn/SBA-15 catalyst	90
Table 4.6	Catalytic activity of 10Cu/SBA-15 and 10ZnO/SBA-15 for CH_3OH synthesis from CO_2 hydrogenation. Reaction conditions: P= 4.0 MPa; T= 250 °C; GHSV= 2400 h^{-1}	92
Table 4.7	BET surface area of calcined SBA-15, 10Cu/10ZnO/SBA-15, and 10ZnO/10Cu/SBA-15	97
Table 4.8	The catalytic activity of different catalysts in CO_2 hydrogenation to CH_3OH. Reaction conditions: P= 4.0 MPa; T= 250 °C; GHSV= 2400 h^{-1}	104
Table 4.9	BET surface area of calcined SBA-15, 5Cu/10ZnO/SBA-15 11Cu/10ZnO/SBA-15 and 20Cu/10ZnO/SBA-15	113
Table 4.10	EDX analysis of 5Cu/10ZnO/SBA-15, 11Cu/10ZnO/SBA-15, 15Cu/10ZnO/SBA-15, and 20Cu/10ZnO/SBA-15	114

Table 4.11 BET surface area of 5Cu/4ZnO/SBA-15, 5Cu/15ZnO/SBA-15, 5Cu/20ZnO/SBA-15 123
Table 4.12 EDX analysis of 5Cu/4ZnO/SBA-15, 5Cu/11ZnO/SBA-15, 5Cu/15ZnO/SBA-15, and 5Cu/20ZnO/SBA-15 124
Table 4.13 Catalytic activity of CO_2 hydrogenation to CH_3OH over various heterogeneous catalysts 131
Table 4.14 Activation energies of CO_2 hydrogenation to CH_3OH and CO over Cu based catalysts 149

LIST OF FIGURES

Page

Figure 1.1 GHGs emission by gas in 2011 (IPCC, 2011) 2

Figure 1.2 Sources of CO_2 emission, Tg CO_2 Eq = million metric tons CO_2 equivalent (IPCC, 2011) 4

Figure 2.1 General steps for SBA-15 formation (Xie et al., 2007) 18

Figure 2.2 Reflux system for (A) industrial distillation colum, (B) lab scale (Wikipedia, 2013) 27

Figure 2.3 Details formulation, other names and properties of CH_3OH (Wikipedia, 2013) 31

Figure 2.4 Cycle of CH_3OH as an alternative fuel 32

Figure 2.5 Products use CH_3OH as a raw material (Methanol holdings, 2013) 33

Figure 2.6 CO_2 phase corresponding to pressure and temperature (Wikimedia commons, 2013) 34

Figure 2.7 Detail formulation, properties, and other names of CO_2 (Wikipedia, 2013) 35

Figure 2.8 CO_2 hydrogenation mechanism on Cu/ZnO catalyst proposed by ab initio MO calculations (Kakumoto and Watanabe, 1997) 38

Figure 3.1 Flowchart of overall experimental work involved in this study 51

Figure 3.2 The overall procedure for synthesis of SBA-15 54

Figure 3.3 The overall synthesis procedure for Cu/SBA-15 and ZnO/SBA-15 55

Figure 3.4 The overall synthesis procedure for bimetallic SBA-15 catalysts 56

Figure 3.5 Schematic diagram of high pressure continuous flow microreactor system 60

Figure 3.6 Photograph of the experimental set-up for hydrogenation of CO_2 to CH_3OH 61

Figure 3.7 Detail representation of the microreactor system 63

Figure 3.8 Schematic diagram of the fixed bed reactor 64

Figure 4.1 XRD patterns of calcined SBA-15 (A) low angle and (B) wide angle 75

Figure 4.2 (A) Adsorption and desorption isotherm of calcined SBA-15 and (B) pore size distribution of calcined SBA-15 77

Figure 4.3 TEM image of calcined SBA-15 from front and side (inset) 78

Figure 4.4 SEM image of calcined SBA-15 79

Figure 4.5 TGA curve of calcined SBA-15 80

Figure 4.6 TEM image of (A) Cu particle, (B) 10Cu/SBA-15 and (C) B zoom image 84

Figure 4.7 TGA analysis of Cu and 10Cu/SBA-15 85
Figure 4.8 (A) CO_2 conversion and (B) CH_3OH STY of Cu and 10Cu/SBA-15 catalyst Reaction conditions: P= 4.0 MPa; T= 250 °C; GHSV= 2400 h^{-1}; t= 5 h 87
Figure 4.9 TEM image of 10ZnO/SBA-15 89
Figure 4.10 H_2-TPR profiles of the 10Cu/SBA-15 and 10ZnO/SBA-15 91
Figure 4.11 Low angle XRD patterns of calcined SBA-15, 10Cu/10ZnO/SBA-15 and 10ZnO/10Cu/SBA-15 95
Figure 4.12 Wide angle XRD patterns of calcined SBA-15, 10Cu/10ZnO/SBA-15 and 10ZnO/10Cu/SBA-15 96
Figure 4.13 N_2 adsorption and desorption isotherm of 10Cu/10ZnO/SBA-15, and 10ZnO/10Cu/SBA-15 98
Figure 4.14 Pore size distribution of 10Cu/10ZnO/SBA-15 and 10ZnO/10Cu/SBA-15 99
Figure 4.15 SEM image of (A) 10Cu/10ZnO/SBA-15 and (B) 10ZnO/10Cu/SBA-15 100
Figure 4.16 TEM micrograph of the (A) 10Cu/10ZnO/SBA-15 and (B) 10ZnO/10Cu/SBA-15 101
Figure 4.17 TGA analysis of 10Cu/10ZnO/SBA-15 and 10ZnO/10Cu/SBA-15 102
Figure 4.18 H_2-TPR profile of 10Cu/10ZnO/SBA-15 103
Figure 4.19 Reaction mechanism for CH_3OH synthesis from CO_2 hydrogenation over novel Cu/ZnO/SBA-15 catalyst 109
Figure 4.20 Wide angle XRD patterns of 5Cu/10ZnO/SBA-15 11Cu/10ZnO/SBA-15, 15Cu/10ZnO/SBA-15 and 20Cu/10ZnO/SBA-15 112
Figure 4.21 N_2 adsorption-desorption isotherm of 5Cu/10ZnO/SBA-15, 11Cu/10ZnO/SBA-15, and 20Cu/10ZnO/SBA-15 113
Figure 4.22 SEM images of (A) 5Cu/10ZnO/SBA-15, (B) 11Cu/10ZnO/SBA-15, (C) 15Cu/10ZnO/SBA-15, and (D) 20Cu/10ZnO/SBA-15 115
Figure 4.23 TEM images of (A) 5Cu/10ZnO/SBA-15 and (B) 20Cu/10ZnO/SBA-15 117
Figure 4.24 The CO_2 conversion and products yield and selectivity obtained over 5Cu/10ZnO/SBA-15, 11Cu/10ZnO/SBA-15, 15Cu/10ZnO/SBA-15, and 20Cu/10ZnO/SBA-15. Reaction conditions: P= 4.0 MPa; T= 250 oC; GHSV= 2400 h-1 118
Figure 4.25 The CH_3OH STY of 5Cu/10ZnO/SBA-15, 11Cu/10ZnO/SBA-15, 15Cu/10ZnO/SBA-15, and 20Cu/10ZnO/SBA-15. Reaction conditions: P= 4.0 MPa; T= 250 °C; GHSV= 2400 h^{-1} 119

Figure 4.26 Wide angle XRD patterns of 5Cu/4ZnO/SBA-15, 5Cu/11ZnO/SBA-15, 5Cu/15ZnO/SBA-15 and 5Cu/20ZnO/SBA-15 122
Figure 4.27 SEM images of (A) 5Cu/4ZnO/SBA-15, (B) 5Cu/11ZnO/SBA-15, (C) 5Cu/15ZnO/SBA-15, and (D) 5Cu/20ZnO/SBA-15 125
Figure 4.28 TEM images of (A) 5Cu/15ZnO/SBA-15 and (B)5Cu/4ZnO/SBA-15 126
Figure 4.29 CO_2 conversion and products yield and selectivity of 5Cu/4ZnO/SBA-15, 5Cu/11ZnO/SBA-15 and 5Cu/20ZnO/SBA-15. Reaction conditions: P= 4.0 MPa; T= 250 oC; GHSV= 2400 h-1 128
Figure 4.30 CH_3OH STY of 5Cu/4ZnO/SBA-15, 5Cu/11ZnO/SBA-15, 5Cu/15ZnO/SBA-15 and 5Cu/20ZnO/SBA-15. Reaction conditions: P= 4.0 MPa; T= 250 oC; GHSV= 2400 h-1 129
Figure 4.31 CO_2 conversion and products yield and selectivity over 5Cu/15ZnO/SBA-15 at reaction pressure of 1.0, 2.5, 4.0, and 5.0 MPa. Reaction conditions: T= 250 oC; GHSV= 2400 h^{-1} 135
Figure 4.32 CH_3OH STY over 5Cu/15ZnO/SBA-15 at reaction pressure of 1.0, 2.5, 4.0, and 5.0 MPa. Reaction conditions: T= 250 oC; GHSV= 2400 h^{-1} 136
Figure 4.33 CO_2 conversion and products yield and selectivity over 5Cu/15ZnO/SBA-15 at reaction temperature of 180, 230, 250, and 280 °C. Reaction conditions: P= 4.0 MPa; GHSV= 2400 h^{-1} 138
Figure 4.34 CH_3OH STY over 5Cu/15ZnO/SBA-15 at reaction temperature of 180, 230, 250, and 280 °C. Reaction conditions: P= 4.0 MPa; GHSV= 2400 h^{-1} 139
Figure 4.35 CO_2 conversion and products yield and selectivity over 5Cu/15ZnO/SBA-15 at total GHSV of 480, 1440, 2400, and 3120 h^{-1}. Reaction conditions: P= 4.0 MPa; T= 250 oC 143
Figure 4.36 CH_3OH STY over 5Cu/15ZnO/SBA-15 at total GHSV of 480, 1440, 2400, and 3120 h^{-1}. Reaction conditions: P= 4.0 MPa; T= 250 °C 144
Figure 4.37 ln k versus 1/T for CO_2 hydrogenation to CH_3OH and CO over 5Cu/15ZnO/SBA-15 at different temperatures of 180 °C, 230 °C, 250 °C, and 280 °C. Reaction conditions: P=4.0 MPa, total GHSV=2400 h^{-1} 148

Figure 4.38 Stability of CO_2 conversion and CH_3OH STY over 5Cu/15ZnO/SBA-15 as function of the time. Reaction conditions: P= 4.0 MPa; T= 250 °C; GHSV= 2400 h^{-1}; t= 24 h 151
Figure A1 Gas chromatogram of products 165
Figure A2 CH_3OH calibration curve 166

LIST OF ABBREVIATIONS

BET	Brunauer-Emmett-Teller
BJH	Barrett, Joyner and Halenda
COST	Change one separate factor at a time
EDX	Energy dispersed X-ray
GC	Gas chromatography
GHGs	Greenhouse gases
GHSV	Gas hourly space velocity
GWP	Global warming potential
H_2-TPR	Hydrogen-temperature programmed reduction
MFC	Mass flow controller
P	Pressure
P123	triblock copolymer poly(ethylene glycol)-poly(propylene glycol)-poly(ethylene glycol)
RWGS	Reverse water gas shift
SBA-15	Santa Barbara Amorphous 15
SEM	Scanning electron microscopy
STY	Space time yield
T	Temperature
t	Time
TCD	Thermal conductivity detector
TCP	Tri-block copolymer
TEM	Temperature electron microscopy
TEOS	Tetraethyl orthosilicate
TGA	Thermogravimetric analysis
TOS	Time on stream
wt.%	Weight percentage
XRD	X-ray diffraction

LIST OF SYMBOLS

%	Percentage
µm	Micrometre
Au	Aurum
Ce	Cerium
CH_3OH	Methanol
CH_4	Methane
cm	centi metre
CO	Carbon monoxide
CO_2	Carbon dioxide
Cr	Chromium
Cu	Copper
CuO	Copper oxide
Ea	Activation energy (kJ/mol)
EO	Ethylene oxide
Fe	Ferum
g	gram
Ga	Galium
Ga_2O_3	Galium oxide
h	Hour
H	Hydrogen atom
H_2	Hydrogen
H_2O	Water
k	Rate constant
Kg	kilogram
m	meter
Mg	Magnesium
Mn	Mangan
Mpa	mega pascal
N_2	Nitrogen
N_2O	Nitrous oxide

Ni	Nickel
NiO	Nickel oxide
nm	nanometre
O	Oxygen atom
^oC	Degree celcius
Pd	Palladium
PO	Propylene oxide
R	Ideal gas law constant (8.314 J/mol.K)
Si	Silicon
Ti	Titanium
TiO_2	Titanium oxide
wt.%	Weight percentage
Zn	Zinc oxide
$ZnCO_3$	Zinc carbonate
ZnO	Zinc oxide
$Zn(OH)_2$	Zinc hydroxide
ZrO_2	Zirconium oxide
θ	Diffraction angle

SINTESIS, PENCIRIAN DAN PELAKSANAAN BERMANGKIN Cu/ZnO/SBA-15 BAGI PENGHIDROGENAN KARBON DIOKSIDA KEPADA METANOL

ABSTRAK

Karbon dioksida (CO_2) adalah gas rumah hijau yang utama yang menyebabkan kepanasan sejagat. Penukaran CO_2 kepada metanol (CH_3OH) adalah salah satu alternatif kepada mahalnya perampasan CO_2 kaji bumi dan samudera. CH_3OH adalah satu bahan penting dalam industri kimia dan dikenali sebagai satu bahan bakar alternatif. Penukaran CO_2 bermangkin dan masa ruang hasil metanol (STY) adalah bagaimanapun dilaporkan sangat rendah. Oleh itu penting untuk membangunkan mangkin secara meningkatkan sifat-sifat penambahan bermangkin. Amorfus Santa Barbara 15 (SBA-15) dengan struktur heksagon yang sangat tersusun, diameter liang (~5.5 nm) dan morfologi zarah yang sekata, ketebalan dinding yang tebal (3.0 to 5.0 nm), luas kawasan permukaan, dan tinggi kestabilan haba telah berjaya disintesis sacara lazim tanpa proses penuaan hidrotermal. SBA-15 yang disintesis digunakan sebagai penyokong mangkin. Beberapa mangkin monologam dan dwilogam kuprum (Cu) atau/dan zink oxida (ZnO) disokong atas SBA-15 telah disintesis secara refluks. Sifat-sifat kimia fizik mangkin yang disediakan dikaji melalui pembelauan X-ray (XRD), penjerapan nitrogen, analisis pemetaan gravity haba (TGA), mikroskop elektron imbasan (SEM), analisis serakan tenaga X-ray (EDX), mikroskopi elektron transmisi (TEM), and hidrogen-penurunan berprogramkan suhu (H_2-TPR). Nilai optimum 5 wt.% Cu dan 15 wt.% ZnO disokong atas SBA-15 digelarkan sebagai 5Cu/15ZnO/SBA-15 dijumpai berkesan untuk memangkinkan penghidrogenan CO_2 kepada CH_3OH. Keadaan optimum proses penghidrogenan CO_2 kepada CH_3OH atas 5Cu/15ZnO/SBA-15 dijumpai pada tekanan tindak balas 4.0 MPa, suhu tindak balas 250 °C, dan halaju ruang jam jumlah gas bahan tindak balas (GHSV) 2400 h^{-1} yang memberi keputusan kepada 22.9% dan 11796.8 mmol $kgcat^{-1}$ h^{-1} masing-masing kepada penukaran CO_2 dan CH_3OH STY. Satu mekanisme laluan sintesis CH_3OH dan tindak balas anjakan balikan gas air (RWGS) atas Cu/ZnO/SBA-15 dicadangkan, berdasarkan keputusan ujikaji yang diperolehi dalam pembelajaran ini. Pengiraan tenaga pengaktifan sintesis CH_3OH dan pembentukan karbon monoksida (CO) adalah masing-masing 35.29 kJ/mol dan 68.02 kJ/mol, Penukaran CO_2 dan CH_3OH STY adalah stabil sepanjang 24 jam arus tindak balas dan didapati tiada nyahaktifan yang ketara. Aktiviti bermangkin tertinggi diperoleh melalui mangkin 5Cu/15ZnO/SBA-15 boleh dihubungkan kepada tingginya serakan Cu dan ZnO keatas permukaan SBA-15, menghasilkan jumlah tapak aktif yang lebih banyak, yang diperlukan untuk sintesis metanol. Pengendapan ZnO penghijrahan diatas permukaan Cu dijumpai untuk nyahaktif tindakbalas RWGS kepada CO; dan oleh itu meningkatkan kememilihan CH_3OH.

SYNTHESIS, CHARACTERIZATION AND CATALYTIC PERFORMANCE OF Cu/ZnO/SBA-15 FOR HYDROGENATION OF CARBON DIOXIDE TO METHANOL

ABSTRACT

Carbon dioxide (CO_2) is the primary greenhouse gas that causes global warming. The conversion of CO_2 into methanol (CH_3OH) is an alternative to the costly geological and oceanic CO_2 sequestration. CH_3OH is an important feedstock in the chemical industries and known as an alternative fuel. The catalytic CO_2 conversion and CH_3OH space time yield (STY) is however reported to be considerably low. It is therefore of importance to develop novel catalysts with improved properties for catalytic growth. Santa Barbara Amorphous 15 (SBA-15) with highly ordered hexagonal structure, uniform pore diameter (~5.5 nm) and particle morphology, thicker wall-thickness (3.0 to 5.0 nm), high surface area (585.20 m^2/g) and high thermal stability was successfully synthesized by the conventional method without hydrothermal aging process. The synthesized SBA-15 was used as catalyst support. A number of monometallic and bimetallic catalyst of copper (Cu) or/and zinc oxide (ZnO) supported on SBA-15 were synthesized by simple reflux method. The physicochemical properties of the as-prepared catalysts were investigated by X-ray diffraction (XRD), nitrogen adsorption, thermogravimetric analysis (TGA), scanning electron microscopy (SEM), energy dispersive X-ray analysis (EDX), transmission electron microscopy (TEM), and hydrogen-temperature programmed reduction (H_2-TPR). The best amount of 5 wt.% Cu and 15 wt.% ZnO supported on SBA-15 designated as 5Cu/15ZnO/SBA-15 was found to effectively catalyze the hydrogenation of CO_2 to CH_3OH. The best process conditions for CO_2 hydrogenation to CH_3OH over 5Cu/15ZnO/SBA-15 were found to be the reaction pressure of 4.0 MPa, the reaction temperature of 250 °C, and the reactants total gas hour space velocity (GHSV) of 2400 h^{-1} that resulted to 22.9% and 11796.8 mmol $kgcat^{-1}$ h^{-1} of CO_2 conversion and CH_3OH STY, respectively. A reaction mechanism of CH_3OH synthesis route and reverse water gas shift (RWGS) reaction on Cu/ZnO/SBA-15 was proposed, based on the experimental results obtained in this study. The calculated activation energies of CH_3OH synthesis and carbon monoxide (CO) formation were 35.29 kJ/mol and 68.02 kJ/mol, respectively. The CO_2 conversion and CH_3OH STY were stable during 24 h of reaction on stream and no obvious deactivation was observed. The higher catalytic activity obtained over the novel 5Cu/15ZnO/SBA-15 catalyst can be correlated to the high dispersion of Cu and ZnO on the SBA-15 surfaces, creating greater amount of Cu-ZnO active sites, which are necessary for CH_3OH synthesis route. The deposited ZnO migration on the Cu surfaces was found to deactivate the RWGS reaction to form CO; and therefore increasing the CH_3OH selectivity.

CHAPTER 1

INTRODUCTION

1.1 Global warming

Global warming is referring to gradual increase in the earth's atmosphere and ocean average temperature. This phenomenon has occurred over the past 100 years and currently is still being one of the major environmental problems. Scientists from the global warming research declared that the global warming has increased the earth average temperature between 0.4 to 0.8 °C and it is predicted to increase up to 1.4 to 5.8 °C over the next hundred years (Livescience, 2013). The evidences of earth warming can be seen by changes in weather and climate. More floods, droughts, intense rain, severe heat waves and other climates related events happen more frequently now. Big changes can be seen in glaciers and oceans, where the ocean are warming and becoming more acidic, ice caps are melting and sea level are rising (EPA, 2013). The most recent report of National Oceanic and Atmospheric Administration (NOAA) stated that the global average temperature in May 2013 was among the top three warmest months of May in past 130 years (NOAA, 2013).

The global warming has been created by greenhouse gases (GHGs) that are capable of absorbing infrared radiation, thereby trapping and holding heat in the atmosphere. Records from total GHGs emissions in 2011 show that the largest contributor is carbon dioxide (CO_2), followed by methane (CH_4), nitrous oxide (N_2O) and several other fluorine-containing halogenated substances (HFCs, PFCs, SF_6) with emissions of 83.7, 8.8, 5.3 and 2.2%, respectively as shown in Figure 1.1 (IPCC, 2007). The impact of GHGs on global warming depends on three factors: abundance of the gas in the planet, duration of its stay in the atmosphere and its global warming potential (GWP) (EPA, 2013). The GWP of a greenhouse gas is defined as the ratio of the timeintegrated radiative forcing from the direct release of 1 kg of a trace substance relative to that of 1 kg of a reference gas (IPCC, 2001). CO_2 has a major impact because of its abundance and ability to stay in the atmosphere up to thousands of years. CH_4 can stay in the atmosphere about 10 years and its GWP is 21 times than that of CO_2. Meanwhile, GWP of N_2O is 310 and its atmospheric lifetime is 114 years. In case of fluorinated gases (HFCs, PFCs, and SF_6), their high heat trapping capacity makes them potential gases contributing to global warming, although they present in very small concentrations (IPCC, 2001; EPA, 2013).

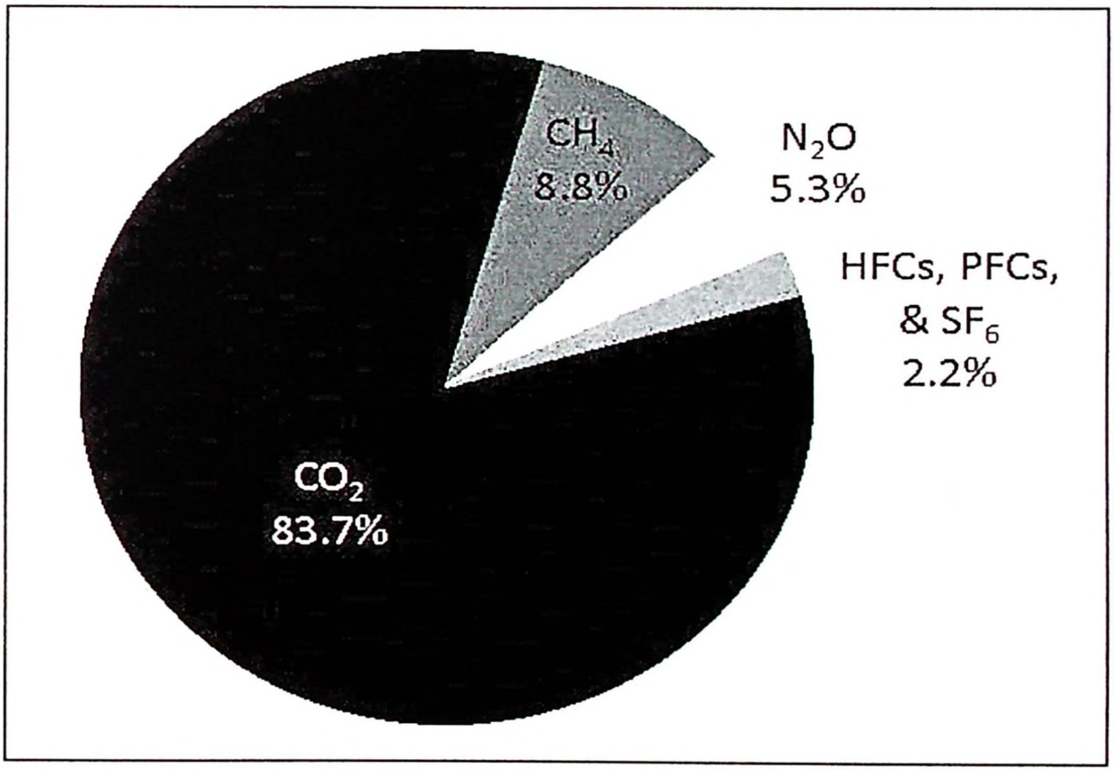

Figure 1.1: GHGs emission by gas in 2011 (IPCC, 2011).

The natural atmospheric concentrations of GHGs have changed by human activities parallel with the growth of energy consumption, transportation, man-made materials and technology (IPCC, 2007; NOAA, 2013). The largest source of CO_2, and overall greenhouse gas emissions, is fossil fuel combustion and its consumption has increased since the industrial revolution; around 270 years ago (Bill et al., 1997). CH_4

emissions are primarily resulted from domestic livestock, agricultural activities, coal mining, and decomposition of wastes in landfills. Agricultural soil management, mobile source fuel combustion and stationary fuel combustion are the major sources of N_2O emissions. Semiconductor manufacturing, primary aluminium production by-product, and electrical transmission and distribution systems are the primary contributors to fluorinated compounds emission (Song, 2006).

1.2 CO_2 in atmosphere

CO_2 is considered as an important ingredient in the carbon cycle of the earth and in the ecological system for plants and animals life, since it is used as carbon source in photosynthesis process and in food production. However, the abundance of CO_2 is more than carbon cycle demand which has led to environmental pollution. The level of CO_2 concentration in the atmosphere has been increasing significantly from decade to decade since 1955 and the most recent data of atmospheric CO_2 are 399.89 ppm for May 2013 (NOAA 2013, EPA, 2013). In addition to fossil-fuel combustion, several other sources emit significant quantities of CO_2. These sources are not limited to non-energy use of fuels but also iron and steel production and cement production (Figure 1.2).

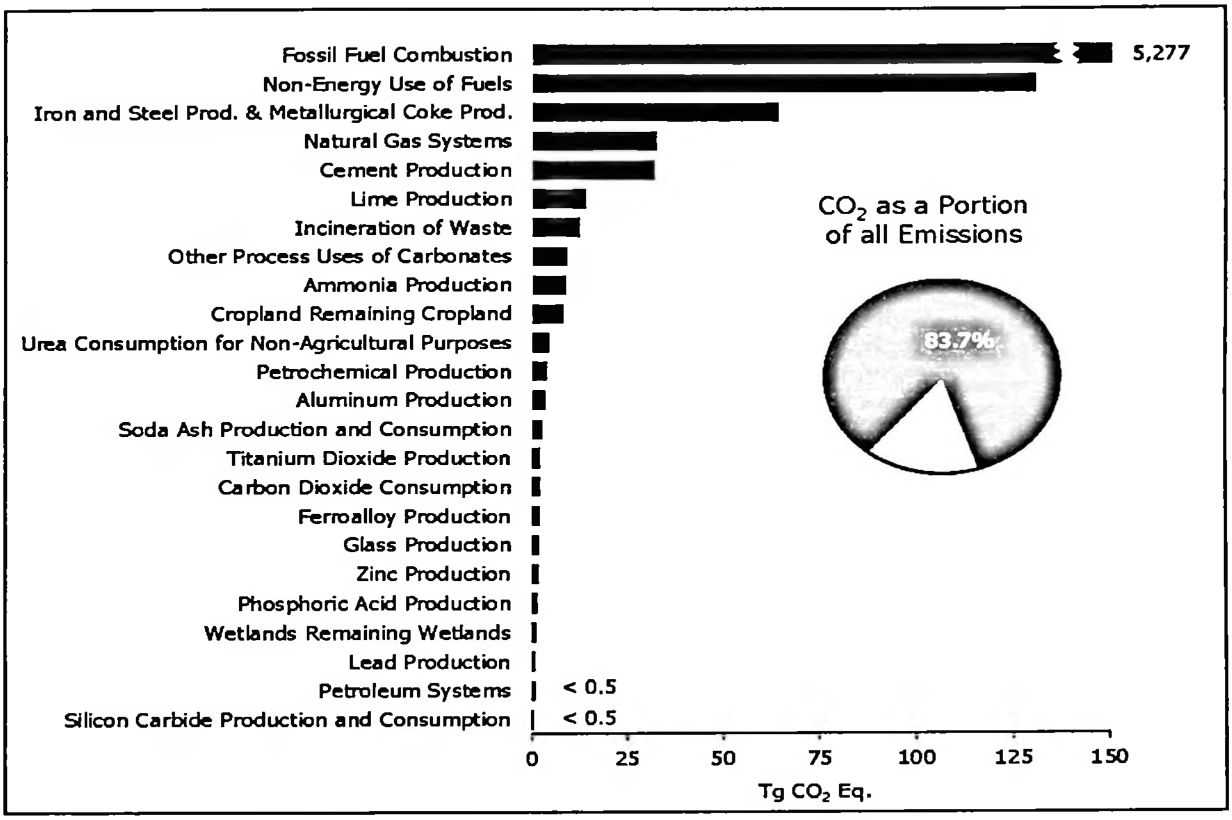

Figure 1.2. Sources of CO_2 emissions, Tg CO_2 Eq. = million metric tons CO_2 equivalent (IPCC, 2011).

1.3 CO_2 conversion for global sustainability

Reducing the CO_2 concentration and emission in the atmosphere is among the most important concerns for environmental protection and also global climate change. Under this circumstance, revolutionary approaches with innovative ideas are needed for green living environment as long term solution. The use of CO_2 as feedstock for producing chemicals is not only interesting for mitigation of GHGs emission, but is an interesting challenge to explore new concepts and opportunities for catalysis and industrial chemistry. Products that can be made from CO_2 include methanol, synthetic gas, dimethyl ether, ethylene, propylene, dimethyl carbonate, cyclic carbonate, and a variety of others (Alizadeh et al., 2009; Lee et al., 2008; Lu et al., 2004; Ma et al., 2009; Ramin et al., 2005; Zhang et al., 2006).

However, there are serious constrains for CO_2 conversion and utilization including relatively high thermodynamic stability of CO_2 molecule, cost of the reaction process, market size limitation, and more energy consumption during the process (Mkhalid, 2014; Naeem et al., 2014; Torrente-Murciano et al., 2014; Zhong et al., 2014). Therefore, the carbon dioxide-based reactions must have high efficiency with enhanced yield and selectivity using lower energy reaction.

1.4 CO_2 hydrogenation to CH_3OH

Since CH_3OH can be used as a starting feedstock in chemical industries and as an alternative to fossil fuels (Fujita et al., 2001; Pipitone and Bolland, 2009; Toyir et al., 2001), therefore it will be interesting to produce CH_3OH from hydrogenation of CO_2. This strategy has been considered as one of the efficient and economical ways that contribute to both fossil fuel substitution and CO_2 emission reduction (Gao et al., 2013). Under proper condition, CH_3OH can be produced via hydrogenation of CO_2 with reverse water gas shift (RWGS) reaction as side reaction (Ma et al., 2009).

CH_3OH formation:

$$CO_2 + 3H_2 \rightarrow CH_3OH + H_2O \qquad (1.1)$$

RWGS reaction:

$$CO_2 + H_2 \rightarrow CO + H_2O \qquad (1.2)$$

CO_2 hydrogenation to CH_3OH over various heterogeneous catalysts has been reported extensively in literatures (An et al., 2009; Ma et al., 2009; Toyir et al., 2001). Up to now, most of the catalysts employ ZnO and Cu as main active component to enhance the reaction yield (Li et al., 2011). However, the activities are still very low with the highest activity reported in literature was 21.0% and 5649 mmol $kgcat^{-1}$ h^{-1} of

CO_2 conversion and space time yield (STY) of CH_3OH, respectively (Sloczynski et al., 2004). Thus, researchers have tried to develop appropriate catalytic systems using different supports, different preparation methods or addition of other active components.

1.5 Santa Barbara Amorphous 15 (SBA-15)

Santa Barbara Amorphous 15 (SBA-15) is one of the promising mesoporous silica materials for various applications. This material was successfully synthesized in early 1990s from independent research groups from Japan and USA. Since the first discovery of SBA-15 preparation, it has been explored and published in almost every issue of catalysis, separation, adsorption, water purification, environmental technology and drug delivery journals (Karvan and Atakül, 2008; Linton et al., 2010; Shah et al., 2007; Wang et al., 2005).

SBA-15 has large surface area, large pore size, and thick walls. It possesses a hexagonal array with tuneable pore diameters in the range of 6.0-20 nm, which is much larger than the 3.0 nm pores which is characteristic of other mesoporous silica of MCM-41 and MCM-48 (Bagshaw and Bruce, 2008). SBA-15 wall thickness is an important parameter for providing a high degree of thermal stability and improved mechanical stability compared to other mesoporous silica. Since the hydrogenation of CO_2 to produce CH_3OH need to be performed at high temperature and pressure, therefore SBA-15 could be a potential candidate to be used in this research work as catalyst support for ZnO and Cu metal components to be deposited.

1.6 Problem statement

Mitigating the atmospheric accumulation of GHGs as the main contributor to global warming is getting worldwide attention nowadays. Kyoto Protocol and Copenhagen Accord have successfully created a strong awareness among the public.

The main objective is to reduce the GHG concentration in the atmosphere at a level that would prevent dangerous anthropogenic interference with the climate change. Besides, Prime Minister of Malaysia, Dato' Seri Najib Tun Razak, said that Malaysia has agreed to cut the nation's CO_2 emission up to 40 % in terms of emission intensity of gross domestic product (GDP) by year 2020 relative to emissions in year 2005 (Mysinchew, 2013).

To address this issue, several approaches have been suggested such as increasing the energy conversion efficiency, turning to less carbon intense fuels, and using renewable energies in human daily activities. However, these strategies may not be enough to sustain the environments impact from global warming in the long term. Therefore, multi-disciplinary and technological approaches towards mitigation of CO_2 are needed. Since the CO_2 disposal process are costly, thus utilizing the CO_2 for production of useful chemicals such as alcohol, syngas, cyclic carbonate and dimethylcarbonate has attracted much attention nowadays.

CO_2 hydrogenation for CH_3OH production is one of the approaches in reducing the CO_2 emission to the atmosphere. CH_3OH is considered as an alternative for fossil fuel and common starting feedstock for chemical industries (Fujita et al., 2001; Nieskens et al., 2011; Pipitone and Bolland, 2009; Toyir et al., 2001). Previously, most researchers conducted the catalytic conversion of CO_2 to CH_3OH through dual steps process which started from CO_2 reforming to syngas, followed by CO_2 hydrogenation to CH_3OH (Nieskens et al., 2011). Then, the developing alternative route was found to produce CH_3OH via single step reaction from CO_2 and hydrogen using high pressure reactors. In long term, this process has seen to save cost, energy and time.

The major constrain in converting CO_2 is the relatively high thermodynamic stability of the molecule itself. In CO_2 hydrogenation, there is a thermodynamic equilibrium competition between the CH_3OH synthesis and RWGS side reaction. The equilibrium state in RWGS can be achieved faster compared to CH_3OH production which could reduce the CH_3OH yield. Meanwhile, other undesired by-products such as hydrocarbons and higher alcohols are usually formed during the reaction. Under this circumstance, most researchers have attempted to examine various catalysts and reactor designs to overcome all these barriers and obtain high CO_2 conversion and CH_3OH production yield.

Highly efficient catalyst is the key factor for CH_3OH synthesis via CO_2 hydrogenation. To date, the exploitation of the catalyst is still not fully satisfactory for industrial application due to the lacking of the essential knowledge in designing the catalyst and control of appropriate catalytic properties for CO_2 hydrogenation. The majority of the catalysts for CO_2 hydrogenation contained Cu and Zn as the main components together with different modifiers and supports (Zr, Ga, Si, Al, Cr, Ce, V, Ti, etc.) (An et al., 2009; Arena et al., 2007; Gao et al., 2012; Guo et al., 2011; Lee et al., 1998; Sloczynski et al., 2004). However, the outcomes from their work still consider as low activity.

Concerning the catalyst properties, the low activity are suggested due to several factors such as: (i) poor dispersion of Cu and Zn particles (Ma et al., 2009), (ii) the stability of the Cu particles (Toyir et al., 2009), (iii) lower surface area of the support material (An et al., 2009), (iv) ability of catalyst to create active sites on the catalyst surfaces (Kusama et al., 2000), and (v) long term stability during the reaction (Sloczynski et al., 2006). Thus, highly challenging approaches are required, not only in the catalysis synthesis but also in the operation to activate the CO_2 molecule and enhance the CH_3OH yield.

In this study, mesoporous SBA-15 is chosen as a support material for Cu and ZnO to be deposited on and was the synthesis catalyst is designated as Cu/ZnO/SBA-15. The SBA-15 properties of higher surface area with well-ordered hexagonal array are expected to provide a proper surface for Cu and ZnO to be deposited and increase the surface area of catalyst. The stability of the Cu and ZnO is expected to enhance by combining with the SBA-15, due to the thicker wall thickness of SBA-15. The well dispersion of Cu and synergetic effect between the active sites and support are expected to stimulate great interest in reaction and nature of active sites. Meanwhile, the presents of ZnO is expected to stabilize the Cu and assist the dispersion of Cu on the catalyst surfaces. Therefore, the Cu/ZnO/SBA-15 catalyst synthesized in this study appearances to increase the metal dispersion, stability and active sites, thereby expected to increase activity and stability of the catalyst in the CO_2 hydrogenation to CH_3OH.

The process and kinetic studies are required to design an appropriate catalytic reaction system for CO_2 hydrogenation to produce optimum CH_3OH yield. However, there are still many debates on these issues due to different catalysts and reaction systems used by previous researchers. Since novel catalysts have been used in this study, it is necessary to investigate the effect of various parameters involved in catalysts synthesis, and reaction condition on production of methanol from CO_2. In addition, the reaction mechanisms between the catalyst and reactant gases; CO_2 and H_2, should be investigated.

1.7 Objectives

The objectives of this research are:

1. To synthesize and characterize novel Cu/ZnO/SBA-15 catalysts.
2. To study the catalytic performance of Cu/ZnO/SBA-15 on hydrogenation of CO_2 for CH_3OH synthesis.
3. To propose catalytic reaction mechanism between reactant gases; CO_2 and H_2, on the surface of Cu/ZnO/SBA-15 in CH_3OH production.

4. To optimize the reaction process parameters for production of CH_3OH from CO_2.
5. To study the catalyst stability and activation energy of CH_3OH and CO formation from CO_2 over Cu/ZnO/SBA-15 catalyst.

1.8 Scopes of the work

The research work can be divided into two sections relating to (a) material science and (b) chemical engineering. The first section involves the synthesis of SBA-15 support by simple conventional method without hydrothermal treatment. The loading of bimetallic system of ZnO and Cu on the SBA-15 support was performed using reflux method. Various catalysts were synthesized and the effect of metal and metal loading amount on the SBA-15 support was considered. The textural and morphological properties of the developed catalysts were investigated using comprehensive characterization techniques by XRD, TEM, SEM, EDX, TGA, BET, and H_2-TPR.

The second section of the research covers the catalytic testing of Cu/ZnO/SBA-15 on CO_2 hydrogenation to produce CH_3OH using the high pressure continuous fixed-bed microreactor. The influence of hydrogenation process parameters including pressure, temperature, and total GHSV on the CO_2 conversion and CH_3OH production yield was investigated using change one separate factor at a time (COST) method. The selection of the parameters was based on the previous studies reported in the literature. The second section also covers the deactivation studies of the most efficient Cu/ZnO/SBA-15 catalyst in CO_2 hydrogenation reaction by prolonging the reaction time on stream (TOS) up to 24 h. Deactivation of Cu/ZnO/SBA-15 was deduced from the results of CO_2 conversion and CH_3OH STY during the reaction. The activation energy of CO_2 hydrogenation reaction to CH_3OH and CO was evaluated by varying the temperature of reaction. A mechanism for hydrogenation of CO_2 over Cu/ZnO/SBA-15 catalyst to produce CH_3OH was also proposed.

1.9 Outline of thesis

This thesis is organized according to the following scheme. The current chapter (Chapter 1) provides a brief introduction into the research topic, problem statements, objectives and scopes of the research. Chapter 2 summarized the published literature related to the materials and method for catalyst synthesis, heterogeneous catalysts, and current issues on CO_2 hydrogenation to CH_3OH. This chapter also analyzed, identifying the knowledge gap and conflicting idea and then conclude the discussion of the topic. Chapter 3 addresses details on the synthesis, characterization and performance study of Cu/ZnO/SBA-15 catalyst in CO_2 hydrogenation reaction. The setup of the high pressure continuous flow fixed-bed microreactor system and analysis of products are also presented in this chapter. Chapter 4 presents and discusses the characterization and catalytic study of the Cu/ZnO/SBA-15 on hydrogenation of CO_2 to produce CH_3OH. Detailed explanations on the catalyst stability, activation energy and reaction mechanism are also included in this chapter. Finally, a summary of the discussions of previous chapters and recommendations for future work is stated in Chapter 5.

CHAPTER 2

LITERATURE REVIEW

This chapter covers the literature review on the materials that had been chosen in synthesis the catalyst, method synthesis of catalyst, the properties and application of main reactant and product and heterogeneous catalysts that were used in literatures in the hydrogenation of CO_2 to CH_3OH.

2.1 Santa Barbara Amorphous 15 (SBA-15)

Santa Barbara Amorphous 15 (SBA-15) is one of the mesoporous silica that firstly produced in 1997 at the University of California, Santa Barbara. This mesoporous pore diameters are typically 3 to 4 times larger than zeolites, and can be nanostructured with respect to the pore diameter and/or overall size particles leading to increase its potential new applications (Corma et al., 1998). Since catalyst supports show significant effects on the catalytic performance due to its influences towards metal dispersion and metal-support interaction. Therefore, SBA-15 has received great attention used as a support in various catalytic applications because of its relatively high surface area (up to 1000 m^2/g), high hydrothermal stability, and well-ordered hexagonal structure (5-30 nm) (Chang et al., 2013; Sasidharan et al., 2009). The applications of SBA-15 as catalyst support and used in catalytic gas reactions reported in previous literatures were simply discussed in this section.

Two series of Au/Ti-SBA-15 prepared by either grafting or direct synthesis method and tested in the propene epoxidation to propene oxide was done by Sacaliuc et al., (2007). Grafted-Au/Ti-SBA-15 was achieved a higher propene oxide selectivity of 99.2% and stable in propene epoxidation up to 5 h, while the activity was very low for catalyst prepared via direct synthesis method. The performance of catalyst was due to the different amount of Ti-dispersed in the SBA-15 structure as well as the formed-Au particle size, which were influenced by method synthesis. Amount of Ti was equaled with the theoretical amount and larger Au particle size was observed in Au/Ti-SBA-15 catalyst prepared by grafted method (Sacaliuc et al., 2007).

Grafted synthesis method was also applied in preparation of Au/TiO_2-SBA-15 for propylene epoxidation to propylene oxide by Liu et al., (2011). Ti/Si ratio of 0.05 exhibited highest catalytic activity of 0.52% and 83% of propylene conversion and propylene oxide selectivity, respectively. A very small Au particles (~1.5 nm) deposited on TiO_2 which incorporated in the SBA-15 channel was predominantly be the reason for its catalyst activity. At reaction temperature of propylene epoxidation lower than 150 °C, the catalyst was stable during 4 h time on stream (Liu et al., 2011).

At NiO loading lower than 50 wt.%, aggregated-NiO on the outer surface of SBA-15 and occluded-NiO into SBA-15 pores were employed by heat treatment (HT) and solvent impregnation (SI) method, respectively (Lu and Kawamoto, 2013). They observed that the methanation activity was depended on the NiO loading not the location of NiO particles in the catalyst system. The conversion of produce gas ($CO+CO_2+H_2$) was increased as NiO loading increases and only methane was produced for the catalyst consist of more than 50 wt.% of NiO loading. Moreover, the synthesis method was affected the reaction equilibrium temperature as seen by SI catalyst could achieve the maximum CO_2 conversion at lower temperature than that HT catalyst (Lu and Kawamoto, 2013).

The effective used of SBA-15 as a support for mono-functional and bi functional metallic Cu, Fe, Cr, and Al synthesized by an incipient wetness impregnation was studied (Zhang et al., 2011). The SBA-15 mesoporous structure was preserved although various metals were impregnated. Among the mono-functional catalysts, Cr/SBA-15 showed a progressively increased as the reaction temperature increases with NO conversion achieved to 90% at 600°C. While over bi-functional Cu-Al/SBA-15, complete NO conversion and 97% propene conversion were obtained at reaction temperature of 500°C. The activity performance of catalyst was concluded to be correlated with dispersion, chemical nature, and the redox property of metal which were ascribed to the promotional in deNO*x* activity (Zhang et al., 2011).

The activity and stability of Pd/SBA-15 and Pd/5% $Ce_{1-x}Zr_xO_2$/SBA-15 catalyst for the combustion of methane were evaluated by Yin et al., (2008). High initial methane conversion of ~97% was obtained over the Pd/SBA-15. However, the catalyst showed very poor stability by methane conversion decreased after 20 h on stream and it conversion was progressively dropped to below 80% after 90 h of reaction. Addition of $Ce_{1-x}Zr_xO_2$ on the Pd/SBA-15 based catalyst was significantly increased the activity and stability of catalyst with the complete methane conversion retained essential after over 400 h of reaction. Moreover, the structural hexagonal of SBA-15 was remained before and after the stability tested (Yin et al., 2008).

Recently, numbers of researchers started to use SBA-15 support in CO_2 reforming of methane, which generally operated at temperature of 800°C – 900°C and atmospheric pressure. The presence of SBA-15 could improve the properties of the catalyst due to its high structural stability, unique pore structure and more uniform mesoporous distribution. The catalyst system exhibits the excellent catalytic performance and kept long term activity stability up to 600 h. This is strongly due to the highly dispersed of active sites on the support and strong resistance toward carbon formation, which the main deactivation factors for reforming (Huang et al., 2011a; Huang et al., 2011b; Liu et al., 2009; Wan et al., 2007; Wang et al., 2012).

A series of Ni/Ce-SBA-15 with Ce/Si molar ratio (0-0.08) prepared via the direct hydrothermal synthesis method was reported by Wang et al., (2012). The metals were successfully incorporated into the SBA-15, and possessed high surface area (885 m^2/g) and narrow pore distribution. Highest catalytic activity was obtained by the catalyst of 0.04 Ce/Si molar ratios, which had reached 95% and 92% of the CO_2 and CH_4 conversion, respectively (Wang et al., 2012). This was due to the optimum molar ratios of Ce/Si promoted the smaller size Ni particles formation, and lead to a highly dispersed of Ni particles on the SBA-15 support. Small particle size of Ni catalyst was reported to more active and stable compared to that of large-particle size due to the carbon deposited is favorable on the large Ni particles (Hou et al., 2007; Tomishige et al., 1999; Wang et al., 2012).

Liu et al., (2009) studied on the effect of Ni supported on two different mesoporous SBA-15 and MCM-41 for CO_2 reforming of CH_4. Both catalysts prepared by grafted method exhibit the excellent catalytic performance with more than 90% of CH_4 conversion. However, 5Ni-SBA-15 was observed to be high stability than that of 5Ni-MCM-41 during the catalytic performance up to 72 h. The activity loss of 5Ni-SBA-15 and 5Ni-MCM-41 after 72 h were 1.26% and 28.0%, respectively. The excellent catalytic activity and long term stability of Ni-SBA-15 were concluded due to the high structural stability of SBA-15 and active metal sintering which exhibited the carbon formation (Liu et al., 2009).

Prolonged the catalytic activity of CO_2 reforming of methane up to 720 h over Ni/SBA-15 has been done by Zhang et al., (2006). An excellent stability of catalyst was observed for both CO_2 and CH_4 conversion during 600 h of reaction time on stream at 800 °C. The continuous reaction run up to 710 h resulted in rapid deactivation of catalyst activity with 25 and 50% decreases in CO_2 and CH_4 conversion, respectively. The results were corresponded to the SBA-15 wall and properties that limited the sintering of the Ni species. Improving the Ni confined to the SBA-15 mesoporous channel could also avoided the Ni sintering and increase the catalyst stability (Zhang et al., 2006a). Moreover, the introduction of Ni into SBA-15 does not affect the mesoporous structures of the SBA-15, although the pore and surface properties are decreased. The structure could prevent the aggregation of Ni particles at higher temperature of reaction (Wan et al., 2007; Zhang et al., 2006a).

1%Rh/Ce-SBA-15 with 1/20 of Ce/Si molar ratios was reported to be the most active, selective and stable catalyst for production of hydrogen from CO_2 reforming of ethanol (Wu and Kawi, 2009). Better catalytic activity was due to the existed-surface oxygen species mobility over the surface of catalyst, which was promoted by Ce incorporated in SBA-15 structure. Additionally, the characterization results showed that the hexagonal mesoporous of SBA-15 modified with CeO_2 remain intact after prolonged the reaction more than 24 h and up to 750 °C.

Yang et al., (2011) prepared the Ti-SBA-15 catalyst for photocatalytic CO_2 reduction to formation of CH_4, C_2H_4 and C_2H_6 hydrocarbons. Possible mechanism for photocatalytic CO_2 reduction process over Ti-SBA-15 is proposed in their report (Yang et al., 2011). Recently, synthesis of TiO_2 nanoparticles on the Al-SBA-15 support in supercritical CO_2 were reported to be active for photocatalytic degradation of methylene blue (Chang et al., 2013). The efficient method could enhanced the hyrothermal stability, and specific surface area while creates new acid sites on the catalyst surface, which resulted to the effective adsorption capability.

A highly active and reusable catalyst adenine modified Ti-SBA-15 for the synthesis of cyclic carbonates and alkyl and aryl carbamates from CO_2 and epoxides was reported (Srivastava et al., 2005). The catalyst showed high yields of the products even in the absence of cocatalyst and solvents in the reaction system (Srivastava et al., 2005). The designed catalyst could avoid the hazardous substances formation like phosgene or isocyanate, which was generally generated low temperature and pressure. Fan et al., 2010 grafted the organotin compounds of $(MeO)_2ClSi(CH_2)_3SnCl_3$ on SBA-15 for the direct synthesis of dimethyl carbonate from methanol and CO_2. The activity of the catalysts depended on the structure, crystal size and surface properties of SBA-15. The dimethyl carbonate yield over regenerated catalyst did not decrease after repeated for six runs (Fan et al., 2010).

These successful achievements of SBA-15 used in gas phase reaction specifically in CO_2 are found to be an effective support for CO_2 hydrogenation to CH_3OH studied in this work. The advantageous characteristics of SBA-15 are expected to provide large surface area for achieving high catalyst metal loading and well dispersed metal deposition. Additionally, the loading of metal on the SBA-15 could enhance the catalyst stability during the reaction. The choice of the SBA-15 support also is expected to influence the catalyst activity as the strength interaction between the metal and the support will influence the dispersion of the metal.

2.2 Synthesis method of SBA-15

It has been well established that the structural characteristics of mesoporous SBA-15 could be tunable to suitable properties to be used in various applications (Weng et al., 2009). The method synthesis of SBA-15 has offered the opportunity to address this issue leading to control the surface area, shape and size of the silica particles, the well-defined pore size and surface, pore wall thickness (Chareonpanich et al., 2007). Numerous studies in the literature address the various synthesis method of SBA-15 such as conventional hydrothermal method (Ooi et al., 2004), ultrasonic irradiation treatment (Chareonpanich et al., 2007; Palani et al., 2010), and microwave hydrothermal process (Han et al., 2007; Newalkar et al., 2000).

The synthesis of mesoporous SBA-15 prepared via conventional hydrothermal method has been firstly reported by Zhao et al., 1998, before extensively being used in literature (Kruk et al., 2000; Ooi et al., 2004; Sasidharan et al., 2009). Generally, SBA-

15 was prepared using the tri-block copolymer (denoted as TCP) as a structure-directing agent and tetraethyl orthosilicate (TEOS) as silica sources. The general formation of SBA-15 can be represented by diagram shown in Figure 2.1.

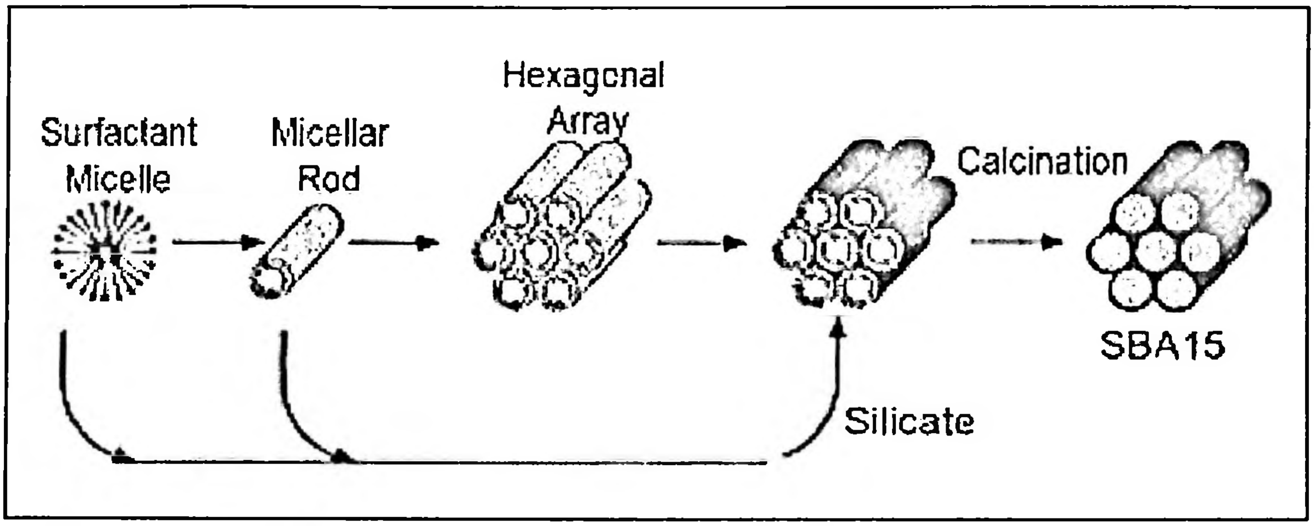

Figure 2.1. General steps for SBA-15 formation (Xie et al., 2007).

Nevertheless, there are some modifications have been made in hydrothermal method to improve the mesoporous structure of SBA-15. Chen et al., 2011 increased the hydrothermal duration to 48 h instead of 24 h. This change was found to reduce the microporosity of the silica structure (Chen et al., 2011). An increased of the synthesis aging temperature led to decrease in complementary pores volume. It was due to the different strength of hydrophobic and hydrophilic properties of the ethylene oxide (EO) and propylene oxide (PO) block co-polymers as the temperature changes (Kruk et al., 2000).

Linton et al., 2010 found that the aggregation characteristic and particle size of SBA-15 could be controlled by adding salts to the ongoing synthesis mixture (Linton et al., 2010). These characteristics depend on the type of salt and the concentration of the salt used. Both cation and anion might be attributed to the interaction of ion polymer inside the mixture which then appeared to be controlling the properties of the mesoporous silica (Linton et al., 2010). The effect of heating rate for calcination mesoporous silica was also studied (Bagshaw and Bruce, 2008). The template removal from the porous structures of SBA-15 appeared to benefit under fast heating rate (20 °C/min) due to the good diffusion access and low combustion temperature of the templates. However, slower heating rate enhanced the pore wall condensation process which then led to flexible formation of silica wall structure (Bagshaw and Bruce, 2008).

Chareonpanich et al., 2007 synthesized the SBA-15 under conventional and ultrasonic treatment (Chareonpanich et al., 2007). As a result, the uniform size of segregate U-shape cylinder particles and aggregate spherical particles were obtained by conventional and ultrasonic treatment, respectively (Chareonpanich et al., 2007). Then, Palani et al., 2010 agreed that the synthesis temperature during the ultrasonic treatment plays an important role in formation of ordered structures. However, prolonged the treatment time more than one hour was not beneficial in enhancing the structures properties of SBA-15 (Palani et al., 2010). This technique can shorten the synthesis time from days to a few hours (Chareonpanich et al., 2007; Palani et al., 2010).

Newalkar et al., 2000 first reported on rapid synthesis of SBA-15 by microwave hydrothermal treatment within 120 min (Newalkar et al., 2000). The method synthesis could increase the pore size and decrease the silica wall thickness due to rapid dehydration of copolymer ethylene oxide (EO) blocks during the microwave treatment (Newalkar et al., 2000). Higher hydrothermal stability of SBA-15 was also successfully synthesized under microwave without presence of any other chemicals (Han et al., 2007). The application of microwave irradiation led to homogeneous nucleation, crystal growth processes and shortens the crystallization time (Han et al., 2007; Newalkar et al., 2000).

Every synthesis methods have their own advantages and weakness towards the SBA-15 characteristics and the process itself. However the technique can be chosen depends on the final characteristics of the SBA-15 aimed, that suitable for the process study. Conventional method without hydrothermal aging stage was chosen in this study to synthesis the SBA-15 support. This method has been used in this study with the aim of synthesizing the suitable characteristics of SBA-15 as well as reducing the preparation time.

2.3 Metallic Copper (Cu) and Zinc Oxide (ZnO)

As well reported in literatures, most of the catalyst system for synthesis of CH_3OH from hydrogenation of CO_2 consist of ZnO and Cu as main components (Arena et al., 2013; Gao et al., 2012; Gao et al., 2013; Guo et al., 2011; Saito et al., 1995). Both Cu and ZnO have their own role in creates the CH_3OH from CO_2 and H_2. Some studies reported that the optimum Cu:ZnO ratio could exhibited the highest catalytic activity (Gao et al., 2013).

2.3.1 ZnO properties and applications

Zinc oxide (ZnO) is an inorganic compound and it is inexpensive, relatively abundant, chemically stable, easy to prepare and non-toxic. It occurs as white hexagonal crystals or a white powder commonly known as zinc white. Recently, Zn is made from purified zinc carbonate ($ZnCO_3$) or zinc hydroxide (ZnOH) by wet chemical processes and then calcined at temperature of 800 °C. On the other hand, indirect process of ZnO is by melted the metallic zinc and vapourize it at temperature around 1000 °C. This causes an instant reaction of zinc vapour with air creating ZnO. The general properties of ZnO are presented in Table 2.1, and the most visible ZnO applications are (Moezzi et al., 2012; International Zinc Oxide Association, 2013; Claus et al., 2012):

(1) As a conductor.

(2) As a semiconductor.

(3) As an additive in numerous materials and products including rubbers, plastics, ceramics, glass, lubricants, cement and many more.

(4) As a gas monitoring devices.

(5) As sensors and biomedical transducers.

(6) In spintronics and smart textiles.

(7) Catalysis.

Table 2.1. Properties of ZnO (Moezzi et al., 2012).

General	
Name, symbol, number	Zinc Oxide, ZnO, 30
Chemical series	Transition metals
Appearance	White solid
Atomic mass	81.408 g/mol
Physical properties	
Phase	Solid
Density	5.606 g.cm-3
Boiling point	2633 K (2360 °C, 4280 °F)
Melting point	2248 K (1975 °C, 3587 °F)

2.3.2 Cu properties and applications

Copper (Cu) is found as native metal and in the minerals cuprite, malachite, azurite, chalcopyrite and bornite. Most Cu is mined or extracted from sulphides, oxides and carbonates minerals and often presence as a by-product in silver production. Cu is amongst the most necessary materials needed to provide the means to keep home, commerce and industry running. This is mainly due to that Cu can be combining with other metals to make new alloys, like brass and bronze. These are harder, stronger and more corrosion resistant than pure copper (Smith et al., 2003; European Copper Institute, 2013). The details properties of Cu are presented in Table 2.2.

The combination of physical properties such as strength, electrical and thermal conductivity, corrosion resistance, machinability, ductility make copper suitable for a wide range of applications including (Copper Development Association, 2013; European Copper Institute, 2013; Smith et al., 2003):

(1) High electrical conductivity.

(2) Construction component.

(3) Core component in wiring of telecommunications system.

(4) Architectural applications.

(5) Core component in transportation industries.

(6) Electronic and related devices.

(7) Antimicrobial applications.

(8) Catalysis.

Table 2.2. Properties of Cu (Smith et al., 2003; Royal society of chemistry, 2014).

General	
Name, symbol, number	Copper, Cu, 29
Chemical series	Transition metals
Group, period, block	11, 4, d
Appearance	Red-orange metallic luster
Atomic mass	63.546 g/mol
Electron configuration	[Ar] $3d^{10}$ $4s^{1}$
Electrons per shell	2, 8, 18, 1
Physical properties	
Phase	Solid
Density	8.96 g.cm-3
Boiling point	2835 K (2562 °C, 4643 °F)
Melting point	1357.77 K (1084.62 °C, 1984.32 °F)
Heat of fusion	13.26 kJ.mol^{-1}
Heat of vaporization	300.4 kJ.mol^{-1}
Heat capacity	24.440 J.mol^{-1}.K^{-1}

2.4 Roles of Cu and ZnO in CH_3OH synthesis from CO_2 hydrogenation

The roles of Cu and ZnO in catalytic activity of CO_2 hydrogenation to CH_3OH synthesis as reported in literatures are briefly addressed in this section. It is well accepted that metallic Cu is the active phase for CH_3OH synthesis via CO_2 hydrogenation (Fujitani and Nakamura, 2000; Guo et al., 2011; Zhao et al., 2011). Its surface area was also responsible for catalytic activity although their relationship sometimes not to be linear (Guo et al., 2011; Guo et al., 2009; Nakamura et al., 1996).

The specific activity for CH_3OH formation was controlled by the ratio of Cu^+/Cu^0 exists on the Cu surface was also reported (Nakamura et al., 1996; Saito et al., 1995). However, Cu alone was only resulted in lower activity in CH_3OH rate formation compared to that catalyst contains of bimetallic Cu and ZnO (Fujitani and Nakamura, 2000).

Xin et al., (2009) addressed that the adsorbed-CO_2 and H_2 was occur on the metallic Cu and ZnO, respectively, and then the CO_2 hydrogenation takes place on the catalyst surface. Some research groups agree with the idea of the optimum dispersion ratio of Cu/ZnO and the number of active species plays an important role in the CO_2 hydrogenation process (Gao et al., 2012; Pillai and Deevi, 2006). The role of Zn to increase the dispersion of Cu particles and create active site species on the catalyst surface seems to be well accepted (Fujitani and Nakamura, 2000; Fujitani and Waugh, 1999).

Some researchers suggested that ZnO could promoted the hydrogen processes by promoted the H_2 spillover onto the Cu surfaces (Fujitani and Nakamura, 2000). Lee et al., (1998) reported that the ZnO seemed to acts as hydrogen storage, which promoted the Cu-formate hydrogenation to CH_3OH. While there are some reports suggested that the activation and spill-over of H_2 were energetic by strong interaction of Cu-ZnO and influences the adsorbed-H_2 on ZnO (Arena et al., 2008; Grunwaldt et al., 2005; Liu et al., 2003; Wilmer et al., 2003). Furthermore, strong Cu-ZnO interaction could enhances the metal particles dispersion, and influences the reactivity and redox properties of the metal Cu phase (Arena et al., 2008).

In numerous studies, the stabilized-Cu^+ ions was reported to be occurred on the surface of ZnO (Nakamura et al., 1996; Sloczynski et al., 2004; Toyir et al., 2001a; Toyir et al., 2001b) This Cu^+ accelerates the dissociative adsorbed-CO_2 on the catalyst surface, which in turn favours the CO_2 hydrogenation. In addition, metallic ZnO itself